PET imaging of somatostatin receptors: design, synthesis and preclinical evaluation of a novel ^{18}F-labelled, carbohydrated analogue of octreotide

H. J. Wester[1], M. Schottelius[1], K. Scheidhauer[1], G. Meisetschläger[1], M. Herz[1], F. C. Rau[1], J. C. Reubi[2], M. Schwaiger[1]

[1] Department of Nuclear Medicine, Klinikum rechts der Isar, Technische Universität München, Ismaningerstrasse 22, 81675 München, Germany
[2] Institute of Pathology, University of Berne, Berne, Switzerland

Received: 19 May 2002 / Accepted: 28 August 2002 / Published online: 5 November 2002

Abstract. Because of the excellent nuclear properties of fluorine-18 and the growing interest in somatostatin receptor (sst) scintigraphy with PET, a novel carbohydrated ^{18}F-labelled sst ligand was developed and preclinically evaluated. Synthesis of N^{α}-(1-deoxy-D-fructosyl)-N^{ε}-(2-[^{18}F]fluoropropionyl)-Lys^0-Tyr^3-octreotate ([^{18}F]FP-Gluc-TOCA) was completed in ~3 h (20%–30% yield). [^{19}F]FP-Gluc-TOCA showed no affinity to hsst1 and hsst3, moderate affinity to hsst4 (IC_{50}: 437±84 n*M*) and hsst5 (IC_{50}: 123±8.8 n*M*) and very high affinity to hsst2 (IC_{50}: 2.8±0.4 n*M*). As a result of carbohydration, lipophilicity of [^{18}F]FP-Gluc-TOCA was found to be low (lg P_{OW}=–1.70±0.02). In mice, the tracer was rapidly cleared via renal excretion (kidneys: 8.69%±1.09%ID/g) and showed low uptake in liver (0.72%±0.14%ID/g) and intestine (1.88%±0.52%ID/g) and high tumour uptake (13.54%±1.47%ID/g) (all data at 1 h p.i.). Tumour to non-tumour ratios at 60 min p.i. reached 25, 19, 7, 1.6 and 56 for blood, liver, intestine, kidney and muscle, respectively. A similar biodistribution pattern was observed in pancreatic tumour-bearing rats. Tumour uptake in rats was reduced to 36% and 18% of control (30 and 60 min) by co-injection of 500 µg Tyr^3-octreotide, demonstrating sst-specific uptake. In a first [^{18}F]FP-Gluc-TOCA-PET study of a patient with a metastatic carcinoid in the liver the tracer showed superior pharmacokinetics, e.g. rapid urinary excretion and low uptake in liver, kidney and spleen. Multiple liver lesions (SUVs ranging from 21.4 to 38.0) and previously unknown focal uptake in the abdomen (SUV 10.0) were clearly visible. This is the first report on PET imaging using an ^{18}F-labelled sst binding peptide; it indicates that [^{18}F]FP-Gluc-TOCA offers excellent imaging characteristics and allows sst imaging with high tumour to non-tumour contrast.

Keywords: Octreotide – Octreotate – Somatostatin – Glycation – Carbohydration – PET

Eur J Nucl Med (2003) 30:117–122
DOI 10.1007/s00259-002-1012-1

H. J. Wester (✉)
Department of Nuclear Medicine, Klinikum rechts der Isar,
Technische Universität München, Ismaningerstrasse 22,
81675 München, Germany
e-mail: H.J.Wester@lrz.tu-muenchen.de
Tel.: +49-89-41404586, Fax: +49-89-41404841

Introduction

Since the late 1980s, strategies for somatostatin receptor (sst) targeted imaging and therapeutic intervention have been intensively investigated. Among the sst ligands investigated, [^{111}In]DTPA-octreotide has been approved for routine clinical scintigraphy of sst-expressing tumours and, more recently, [^{99m}Tc]depreotide has been approved for the evaluation of lung carcinoma. Furthermore, results obtained with sst-targeted peptide receptor radiotherapy (PRRT) are promising, and, for example, [^{90}Y]DOTA-Tyr^3-octreotide and [^{177}Lu]DOTA-Tyr^3-octreotate are being investigated in ongoing clinical radiotherapy trials.

Because of the high spatial resolution of positron emission tomography (PET) and its ability to quantify biodistribution and uptake kinetics, sst ligands have also been labelled with the positron emitters ^{18}F (96.7% β^+), ^{64}Cu (17.4% β^+), ^{66}Ga (56% β^+), ^{68}Ga (89% β^+), ^{76}Br (55.6% β^+), ^{86}Y (31.9% β^+) and ^{124}I (22.8% β^+). The ease of peptide radiolabelling by complexation makes ^{68}Ga ($E_{\beta^+,max}$=2.921 MeV, $t_{1/2}$=67.6 min), which can be obtained from the ^{68}Ge/^{68}Ga generator, and ^{64}Cu (17.4% β^+, $E_{\beta^+,max}$=1.673 MeV, $t_{1/2}$=12.7 h, 39.6% β^-, $E_{\beta^-,max}$=

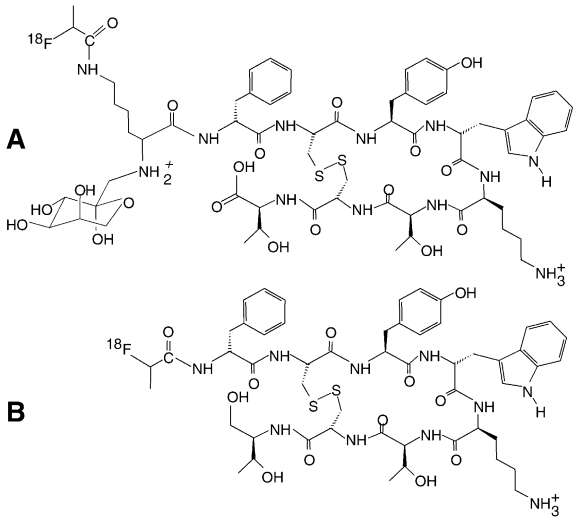

Fig. 1. Structure of the novel sst ligand N^{α}-(1-deoxy-D-fructosyl)-N^{ε}-(2-[^{18}F]fluoropropionyl)-Lys^0-Tyr^3-octreotate ([^{18}F]FP-Gluc-TOCA) (**A**) and the previously described non-carbohydrated analogue 2-[^{18}F]fluoropropionyl-D-Phe^1-octreotide (**B**) [4, 5]

0.579 MeV) interesting radionuclides for routine clinical PET imaging and combined PET/PRRT, respectively. Consequently, [^{66}Ga]DOTA-Tyr^3-octreotide (PET/PRRT) [1], [^{68}Ga]DOTA-Tyr^3-octreotide (PET) [see, e.g. 2] and [^{64}Cu]TETA-octreotide (PET/PRRT) [3] are being evaluated in animals and man.

Experiences with ^{18}F-labelled sst binding peptides are limited and reported results are disappointing. Biodistribution studies of 2-[^{18}F]fluoropropionyl-D-Phe^1-octreotide [4, 5] and 4-[^{18}F]fluorobenzoyl-D-Phe^1-octreotide [6] in rodents revealed low tumour uptake, low tumour retention and unfavourable biokinetics.

Recent studies from our group on the design and optimisation of octreotide analogues [7, 8, 9] and integrin antagonists [10, 11] demonstrated that carbohydrate conjugation can successfully be applied to reduce lipophilicity, plasma protein binding, hepatic uptake, hepatobiliary transfer or unspecific uptake, and to increase tumour uptake and renal excretion. Furthermore, the compounds still showed high affinity to their binding sites.

The goal of the current study was the design, synthesis and preclinical evaluation of a carbohydrated ^{18}F-labelled sst ligand. For this purpose Lys^0-octreotate was synthesised allowing both carbohydration via Maillard reaction and Amadori re-arrangement and ^{18}F-labelling at the N-terminus (Fig. 1). Biodistribution and tumour uptake of the novel PET ligand N^{α}-(1-deoxy-D-fructosyl)-N^{ε}-(2-[^{18}F]fluoropropionyl)-Lys^0-Tyr^3-octreotate ([^{18}F]FP-Gluc-TOCA) was investigated in rat pancreatic tumour (AR42J) xenografted mice and CA20948 tumour-bearing Lewis rats. The affinity profile of [^{19}F]FP-Gluc-TOCA was assessed in cells expressing sst1–sst5. Specificity of tumour uptake was demonstrated in vivo by pretreatment experiments in rats. Here, an initial [^{18}F]FP-Gluc-TOCA PET study in a patient suffering from a metastatic carcinoid in the liver but unknown primary is reported.

Materials and methods

The peptide was synthesised by solid phase synthesis using the Fmoc strategy as described elsewhere [9]. Maillard reaction was used for coupling of glucose to the N-terminus [8, 9]. Synthesis of 4-nitrophenyl 2-[^{18}F]fluoropropionate was carried out according to the literature [4, 5]. For ^{18}F-acylation of N^{α}-(1-deoxy-D-fructosyl)-Lys^0-Tyr^3-Lys^5(Dde)-octreotate the peptide (2 mg) was dissolved in DMSO and added to a vial containing no carrier added (n.c.a.) 4-nitrophenyl 2-[^{18}F]fluoropropionate. The mixture was heated (10 min, 50°C) and subjected to high-performance liquid chromatography (HPLC) [Multospher 100 RP18-5 (250×10 mm; linear gradient 22%–30% B; 15 min; 0.1% trifluoroacetic acid in water (A), 0.1% trifluoroacetic acid in acetonitrile (B), flow rate 5 ml/min, t_R=15–17 min; K´=7]. The detailed synthesis of [^{18}F]FP-Gluc-TOCA will be described elsewhere.

For animal experiments, the product fraction was evaporated to dryness and reconstituted in 0.05 *M* phosphate-buffered saline (pH 7.4). For patient application, the activity was reconstituted in 200 µl EtOH, diluted to a volume of 10 ml with 25 m*M* phosphate-buffered saline (pH 7.4), followed by sterile filtration. Quality control was carried out using an analytical column [Nucleosil 100 5-C18 (125×4.8 mm)] and a linear gradient of 10%–60% B over a period of 15 min (t_R=13.5; K´=8).

Biodistribution studies at 10 and 60 min p.i. were carried out in rat pancreatic tumour (AR42J) xenografted nude mice after administration of 370 kBq of [^{18}F]FP-Gluc-TOCA in 100 µl of phosphate-buffered saline into the tail vein. The pharmacokinetics in CA20948 pancreatic tumour-bearing rats at 45, 90 and 120 min p.i. was determined after intravenous injection of 3.7 MBq of [^{18}F]FP-Gluc-TOCA into the tail vein. To demonstrate sst-specific uptake of the tracer, a further group of rats was treated with a mixture of 3.7 MBq (500 µCi) n.c.a. [^{18}F]FP-Gluc-TOCA and 500 µg TOC/rat and investigated at 30 min (n=2) and 60 min p.i. (n=2); comparison was made with control animals which received only n.c.a. [^{18}F]FP-Gluc-TOCA (30 min, n=2; 60 min, n=3). All experiments were carried out following the principles of laboratory animal care and the German law on the protection of animals. Activity uptake in tissues is expressed in %ID/g tissue (mean±SD). Lipophilicity of the radiopharmaceutical was determined as previously described [8, 9].

Cells stably expressing human sst_1, sst_2, sst_3, sst_4 and sst_5 were grown as previously described [12]. Cell membrane pellets were prepared and receptor autoradiography was performed as previously described in detail [9]. Displacement experiments were performed with the universal sst binder [^{125}I]-[Leu^8, D-Trp^{22}, Trp^{25}]-somatostatin 28 using increasing concentrations of the reference compound [^{19}F]FP-Gluc-TOCA and somatostatin 28 as control (0.1–1,000 n*M*). IC_{50} values were calculated after quantification of the data using a computer-assisted image processing system.

A 72-year-old female patient suffering from a metastatic carcinoid in the liver but unknown primary was studied using an ECAT EXACT 951/R scanner prior to a compassionate radiopeptide therapy. Details of the study were explained to the patient by a physician, and written informed consent was obtained. The axial resolution of the scanner at FWHM (full-width at half-maximum) is approximately 5 mm, and the transaxial resolution 8 mm. Two whole-body scans spanning from the skull to the bladder were per-

formed (six overlapping bed positions, 8 min per position) at 15 min p.i. (15–65 min) and 90 min p.i. (90–140 min) of 107 MBq of [^{18}F]FP-Gluc-TOCA. Images were reconstructed by an attenuation-weighted iterative ordered subsets-expectation maximisation (OSEM) algorithm using eight iterations and four subsets. The image pixel counts were calibrated to activity concentrations (Bq/g), and standardised uptake values (SUVs) were calculated using the formula: SUV=tissue concentration/(injected dose/body weight). Regions of interest were defined and the corresponding SUVs were calculated for the early and late whole-body scan. Two days prior to the PET study the patient underwent a conventional [^{111}In]DTPA-octreotide whole-body planar scintigraphy (1, 4 and 24 h p.i.) using a dual-head gamma camera with medium-energy collimators.

Results

Based on previous studies from our group [7, 8, 9, 10, 11], a trifunctional linker concept was successfully applied to synthesise the carbohydrated ^{18}F-labelled octreotide analogue [^{18}F]FP-Gluc-TOCA. Synthesis of [^{18}F]FP-Gluc-TOCA was completed in about 3 h (EOB, 25%±5% radiochemical yield, radiochemical purity >98%, specific activity >37 GBq/μmol, *n*=8).

Determination of the in vitro binding profile of the reference compound [^{19}F]FP-Gluc-TOCA and natural somatostatin-28 as control to human sst (Table 1) showed no affinity of [^{19}F]FP-Gluc-TOCA to hsst1 and hsst3 (IC_{50}: >1,000 nM), moderate affinity to hsst4 (IC_{50}: 437±84 n*M*) and hsst5 (IC_{50}: 123±8.8 n*M*) and very high affinity to hsst2 (IC_{50}: 2.8±0.4 n*M*).

Compared with N^{α}-(2-[^{18}F]fluoropropionyl)-D-Phe^{1}-octreotide [4, 5], [^{18}F]FP-Gluc-TOCA exhibits reduced lipophilicity (lg P_{OW}=–0.07±0.01 vs –1.70±0.02, respectively) and low uptake in the liver (11.1%±4.6%ID/g vs 0.72%±0.14%ID/g at 1 h p.i.) and intestine (20.0%± 3.7%ID/g vs 1.88±0.52%ID/g at 1 h p.i.) (Table 2).

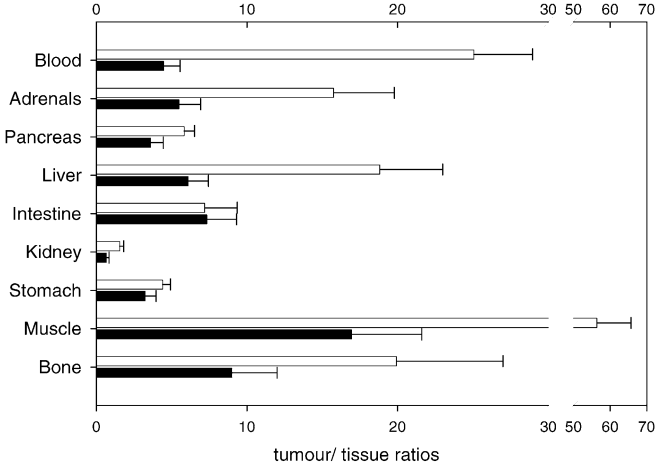

Fig. 2. Tumour/tissue uptake ratios of [^{18}F]FP-Gluc-TOCA in AR42J rat pancreatic tumour xenografted mice 10 min (*black bars*) and 60 min (*white bars*) post injection

Table 1. Affinity profile (IC_{50}) of somatostatin-28 and FP-Gluc-TOCA for human sst1-sst5 receptors [values are IC_{50}±SEM (n*M*), number of experiments in parentheses]

Peptides	sst1	sst2	sst3	sst4	sst5
Somatostatin-28	2.5±0.2 (3)	3.8±0.1 (3)	5±0.9 (3)	2.5±0.7 (3)	3.2±0.5 (3)
[^{19}F]FP-Gluc-TOCA	>10,000 (3)	2.8±0.4 (3)	>1,000 (3)	437±84 (3)	123±8.8 (3)

[^{19}F]FP-Gluc-TOCA: N^{α}-(1-deoxy-D-fructosyl)-N^{ε}-(2-[^{19}F]fluoropropionyl)-Lys^{0}-Tyr^{3}-octreotate

Table 2. Tissue distribution of [^{18}F]FP-Gluc-TOCA in AR42J tumour-bearing mice compared with the biodistribution of 2-[^{18}F]fluoropropionyl-D-Phe^{1}-octreotide [4, 5] in non-tumour-bearing NMRI mice (%ID/g, values are mean±SD)

Organ	[^{18}F]FP-Gluc-TOCA		2-[^{18}F]fluoropropionyl-D-Phe^{1}-octreotide [4]	
	10 min p.i. (*n*=5)	60 min p.i. (*n*=5)	10 min p.i. (*n*=3)	60 min p.i. (*n*=3)
Tumour	11.52±2.44	13.54±1.47	–	–
Blood	2.58±0.31	0.54±0.06	3.0±0.4	0.4±0.1
Liver	1.89±0.11	0.72±0.14	22.3±5.3	11.1±4.6
Intestine	1.57±0.26	1.88±0.52	9.9±1.7	20.0±3.7
Stomach	3.56±0.27	3.07±0.14	–	–
Kidney	17.47±3.32	8.69±1.09	13.5±1.5	2.9±0.2
Pancreas	3.20±0.32	2.32±0.11	3.1±0.2	1.8±0.5
Adrenals	2.10±0.32	0.86±0.20	3.7±1.2	n.d.
Muscle	0.68±0.12	0.24±0.03	–	–
Bone	1.28±0.33	0.68±0.23	2.2±0.3	3.1±0.3

Table 3. Tissue distribution of [^{18}F]FP-Gluc-TOCA in CA 20948 pancreatic tumour-bearing male Lewis rats (%ID/g, values are mean±SD)

Organ	30 min (*n*=3)	45 min (*n*=4)	60 min	90 min (*n*=3)	120 min (*n*=4)
Tumour					
Tracer only	0.791±0.413	1.242±0.775	1.481±0.181 (*n*=3)	0.750±0.428	0.607±0.217
Competition	0.287±0.017	–	0.271±0.044 (*n*=2)	–	–
Percent of control	36.3%±19.1%		18.3%±3.7%		
Blood	–	0.285±0.043	–	0.068±0.011	0.054±0.045
Lung	–	0.245±0.083	–	0.099±0.012	0.092±0.027
Liver	–	0.199±0.063	–	0.079±0.020	0.071±0.013
Spleen	–	0.116±0.069	–	0.043±0.015	0.052±0.019
Pancreas	–	5.926±2.094	–	5.261±1.336	6.137±0.750
Stomach	–	0.660±0.104	–	0.637±0.053	0.500±0.082
Intestine	–	0.829±0.427	–	0.912±0.338	0.338±0.099
Adrenals	–	4.181±0.521	–	4.808±0.923	4.804±0.894
Kidney	–	0.776±0.707	–	0.997±0.205	0.954±0.156
Muscle	–	0.036±0.014	–	0.012±0.004	0.010±0.002
Bone	–	0.055±0.026	–	0.016±0.013	0.016±0.013

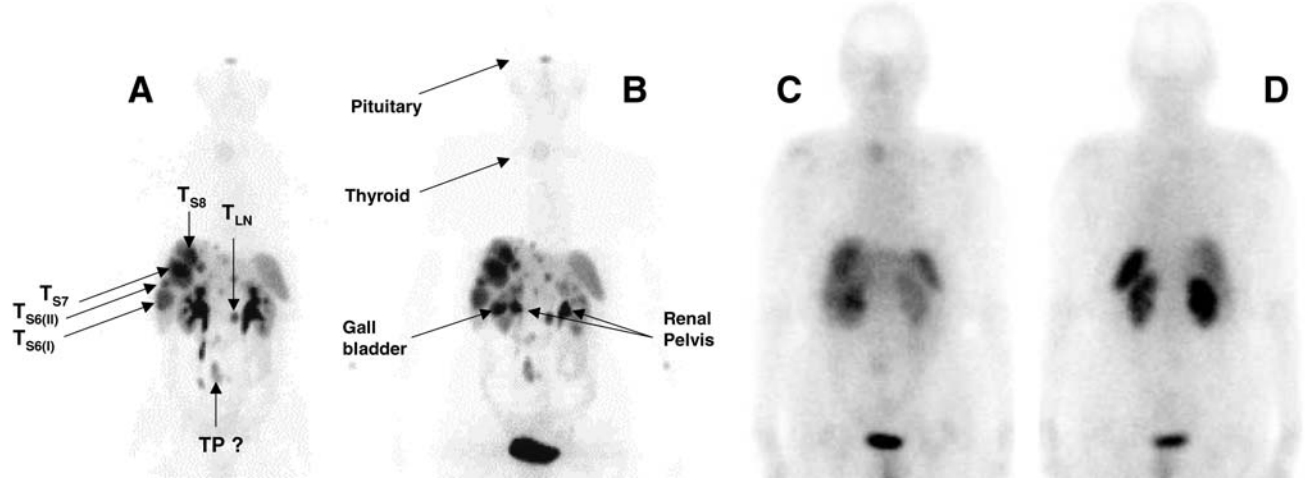

Fig. 3. Maximum intensity projections (whole-body scan **A** 15–65 min p.i. and **B** 90–140 min p.i.) of a 72-year-old female patient suffering from a metastatic carcinoid in the liver and unknown primary after 107 MBq of [^{18}F]FP-Gluc-TOCA. SUVs for the metastases T_{S6}–T_{S8}, the extrahepatic lesion (paravertebral) T_{LN}, a newly detected lesion which presumably represents the primary (TP) tumour and selected organs are listed in Table 4. **C, D** Anterior and posterior planar scintigraphy of the same patient 24 h following the injection of 111 MBq [^{111}In]OcreoScan. The extent and number of liver metastases are unclear, and there is uncertain visualisation of a primary in the middle abdomen

[^{18}F]FP-Gluc-TOCA was rapidly cleared from the blood predominantly by urinary excretion. Thus, kidney uptake was high (17.47%±3.32%ID/g) at 10 min and decreased to 8.69%±1.09%ID/g at 1 h. Accumulation in the adrenals and pancreas known to express ssts reached 0.86±0.20 and 2.32±0.11%ID/g at 1 h. High activity uptake was found for the tumour (13.54%±1.47%ID/g at 1 h p.i) (Table 2). Tumour to non-tumour ratios at 60 min p.i. reached 25, 19, 7, 1.6 and 56 for blood, liver, intestine, kidney and muscle, respectively (Fig. 2). Defluorination in vivo was negligible (bone: 0.7%±1.47%ID/g at 1 h).

A similar biodistribution pattern was observed in the CA20948 pancreatic tumour-bearing rats (Table 3). Most notably, tumour uptake of [^{18}F]FP-Gluc-TOCA reached a maximum at 60 min p.i. Thirty-six percent and 18% of tracer uptake into the tumour at 30 and 60 min p.i. was blocked by co-injection of 500 μg Tyr^3-octreotide (TOC) per rat.

Conventional scintigraphy results obtained in a patient with a history of a histologically proven metastatic carcinoid in the liver showed abnormally high activity uptake in multiple liver lesions (Fig. 3C, D). Due to the limited resolution of single-photon emission tomography

Table 4. Standardised uptake values (SUVs) for comparison of tumour and tissue uptake of [^{18}F]FP-Gluc-TOCA as calculated from early (15–65 min) and late (90–140 min) whole-body imaging (see Fig. 3)

	SUV (early)	SUV (late)
Tumour		
$T_{S6(I)}$	24.9	23.5
$T_{S6(II)}$	21.4	23.8
T_{S7}	38.0	37.9
T_{S8}	34.1	36.7
T_{LN}	19.9	23.1
$T_{Primary}$ (TP)	10.0	9.7
Pituitary	3.6	3.5
Spleen	11.5	10.9
Lung	0.6	0.4
Left kidney	14.1	9.8
Right kidney	13.9	9.5
Gall-bladder	5.9	36.8

(SPET), single metastases in the range 0.5–6 cm previously visible on MRI could not be resolved and were visible as regions of large, pronounced liver uptake. In addition, faint focal uptake was detected in the middle abdomen, presumably representing the primary tumour.

[^{18}F]FP-Gluc-TOCA-PET revealed rapid clearance of the tracer from the blood pool within the first hour p.i. by predominantly renal excretion (Fig. 3A). Multiple liver lesions could clearly be delineated with SUVs of the selected regions of interest depicted in Fig. 3A ranging from 21.4 to 38.0 (Table 4). In addition, intense focal uptake in the area of the coeliac trunk (SUV 29.9) and a less intense focus in the middle abdomen (SUV 10.0) were visible. Sst-specific tracer uptake plateaued within the first hour p.i., as demonstrated by the similar SUVs calculated from the early and late imaging. Whereas the activity cleared from the blood appeared in the kidney in the early image, most of the activity was located in the bladder at 90–140 min p.i. (Fig. 3D). Thus, SUVs calculated for the renal parenchyma at both time points decreased from 14.0±0.2 to 9.5±0.3 (Table 4). Although most of the activity was excreted by the kidney, the appearance of the gall-bladder in the late image (SUV 36.8) revealed hepatobiliary transport of [^{18}F]FP-Gluc-TOCA.

Discussion

The primary objective of this study was to determine whether the pharmacokinetics of ^{18}F-labelled sst targeted PET tracers may be improved by the use of a carbohydrate conjugated octreotide analogue. Previous studies from our group have already demonstrated the effects of carbohydration [7, 8, 9] and sugar amino acid conjugation [10, 11] on the biodistribution and tumour uptake of radioiodinated octreotides and RGD peptides. In this study lysine was chosen as a trifunctional linker in order to combine the prosthetic group bearing the radiolabel, the pharmacokinetics modifier (the carbohydrate) and the sst ligand octreotate. The resulting compound, N^{α}-(1-deoxy-D-fructosyl)-N^{ε}-(2-fluoropropionyl)-Lys^0-Tyr^3-octreotate (FP-Gluc-TOCA) showed very high affinity for hsst2 (IC_{50}: 2.8±0.4), which is similar to the binding affinity of Ga-DOTATOC (IC_{50}: 2.5±0.4). More relevant, however, are the results achieved by the ligand design, i.e. carbohydration. Compared with other radiohalogenated sst ligands recently investigated, and especially the previously evaluated ^{18}F-fluoropropionylated and non-carbohydrated ligand 2-[^{18}F]fluoropropionyl-D-Phe^1-octreotide [4, 5], [^{18}F]FP-Gluc-TOCA exhibits outstanding pharmacokinetics. On the basis of the results obtained in the animal models and in the first human PET study, it can be concluded that the biodistribution of this novel PET tracer closely resembles the biodistribution of known radiometallated ligands, such as Ga-DOTATOC. Thus, rapid activity uptake in the tumour tissue paralleled by fast background clearance and excretion resulted in high contrast. Due to the fast tracer kinetics, the inherent disadvantage of radiohalogenated octreotides, i.e. short tumour retention, seems of less importance within the time period suitable for [^{18}F]FP-Gluc-TOCA PET imaging.

Although preparation of [^{18}F]FP-Gluc-TOCA is carried out by means of a remote-controlled apparatus in quantities sufficient for application in two to four patients, the ease of radiometallation may currently favour compounds such as [^{68}Ga]DOTATOC or [^{64}Cu]TETA-octreotide for PET imaging. Considering the small number of clinically relevant peptides and other tracers suitable for ^{68}Ga or ^{64}Cu labelling, the cost-effective use of a ^{68}Ge/^{68}Ga generator still has to be shown.

We are very optimistic that it will be possible to adapt advances in the development of simplified ^{18}F-fluorination methods for optimisation of the trifunctional linker approach and thus to improve the synthesis of [^{18}F]FP-Gluc-TOCA and corresponding analogues. We assume that the trifunctional linker concept used in this study is a promising strategy for improving pharmacokinetics by variation of the carbohydrate not only for sst ligands but also for other peptide radiopharmaceuticals.

The results obtained in this study indicate that [^{18}F]FP-Gluc-TOCA is a very promising tracer for PET imaging of sst-positive tumours. Further evaluation in a series of patients seems warranted.

Acknowledgements. The authors are indebted to Prof. R. Senekowitsch-Schmidtke and her team for carrying out the biodistribution studies and Jutta Grahneis, Kristin Hoffmann, Brigitte Drzewas and Coletta Kruschke for their excellent technical assistance. Furthermore, we appreciate the editorial help of Jodi Neverve in the preparation of the manuscript. This work was supported by the Deutsche Forschungsgemeinschaft, FOR 411/We 2386/2-1 and FOR 411/Sche 407/4-1.

References

1. Ugur O, Kothari PJ, Finn RD, Zanzonico P, Ruan S, Guenther I, Maecke HR, Larson SM.Ga-66 labelled somatostatin analogue DOTA-DPhe1-Tyr3-octreotide as a potential agent for positron emission tomography imaging and receptor mediated internal radiotherapy of somatostatin receptor positive tumours. *Nucl Med Biol* 2002; 29:147–157.
2. Hofmann M, Maecke H, Borner R, Weckesser E, Schoffski P, Oei L, Schumacher J, Henze M, Heppeler A, Meyer J, Knapp H. Biokinetics and imaging with the somatostatin receptor PET radioligand ^{68}Ga-DOTATOC: preliminary data. *Eur J Nucl Med* 2001; 28:1751–1757.
3. Anderson CJ, Dehdashti F, Cutler PD, Schwarz SW, Laforest R, Bass LA, Lewis JS, McCarthy DW. ^{64}Cu-TETA-octreotide as a PET imaging agent for patients with neuroendocrine tumours. *J Nucl Med* 2001; 42:213–221.
4. Guhlke S, Wester HJ, Bruns C, Stocklin G. (2-[^{18}F]fluoropropionyl-(D)phe1)-octreotide, a potential radiopharmaceutical for quantitative somatostatin receptor imaging with PET: synthesis, radiolabeling, in vitro validation and biodistribution in mice. *Nucl Med Biol* 1994; 21:819–825.
5. Wester HJ, Brockmann J, Rösch F, Wutz W, Herzog H, Smith-Jones P, Stolz B, Bruns C, Stöcklin G. PET-Pharmacokinetics of ^{18}F-octreotide: A comparison with ^{67}Ga-DFO-octreotide and ^{86}Y-DTPA-octreotide. *Nucl Med Biol* 1997; 24:275–286.
6. Hostetler ED, Edwards WB, Anderson CJ, Welch MJ. *J Lab Compd Radiopharm* 1999; 42 Suppl 1:720–722.
7. Leisner M, Kessler H, Schwaiger M, Wester HJ. Synthesis of N^{α}-Amadori-derivatives of Tyr^3-octreotide: precursors for I-123- and F-18-labelled sst-binding SPECT/PET tracers with improved biodistribution. *J Lab Compd Radiopharm* 1999; 42 Suppl 1:549–551.
8. Wester HJ, Schottelius M, Scheidhauer K, Reubi JC, Wolf I, Schwaiger M. Comparison of radioiodinated TOC, TOCA and Mtr-TOCA: the effect of carbohydration on the pharmacokinetics. *Eur J Nucl Med Mol Imaging* 2002; 29:28–38.
9. Schottelius M. Wester HJ, Reubi JC, Senekowitsch-Schmidtke R, Schwaiger M. Improvement of pharmacokinetics of radioiodinated Tyr^3-octreotide by conjugation with carbohydrates. *Bioconjugate Chem* 2002; in press.
10. Haubner R, Wester HJ, Weber WA, Mang C, Ziegler SI, Goodman SL, Senekowitsch-Schmidtke R, Kessler H, Schwaiger M. Noninvasive imaging of alpha(v)beta3 integrin expression using ^{18}F-labelled RGD-containing glycopeptide and positron emission tomography. *Cancer Res* 2001; 61:1781–1785.
11. Haubner R, Wester HJ, Burkhart F, Senekowitsch-Schmidtke R, Weber W, Goodman SL, Kessler H, Schwaiger M. Glycosylated RGD-containing peptides: tracer for tumour targeting and angiogenesis imaging with improved biokinetics. *J Nucl Med* 2001; 42:326–336.
12. Reubi JC, Schaer JC, Waser B, et al. Affinity profiles for human somatostatin receptor sst1–sst5 of somatostatin radiotracers selected for scintigraphic and radiotherapeutic use. *Eur J Nucl Med* 2000; 27:273–282.